DOI: 10.1002/ejic.200701253

Cu^{I}–Br Oligomers and Polymers Involving Cu–S(cystamine) Bonds

Nicolas Louvain,[a] Nicolas Mercier,*[a] and Mohamedally Kurmoo[b]

Keywords: Amines / Disulfides / Copper / Organic–inorganic hybrid composites / Halogens

The syntheses, crystal structures, and thermal properties of five cuprous bromides derived from cystamine, $[NH_3(CH_2)_2SS(CH_2)_2NH_3]^{2+}$, here denoted by (SS), are reported. Whereas $(SS)_2Cu_4Br_8$ (**1**) is a polar tetramer and $(SS)_2Cu_2Br_6$ (**2**) consists of $[(SS)Cu_2Br_6]^{2-}$ dimers, α1-$(SS)Cu_2Br_4$ (**3**), $(SS)Cu_3Br_5$ (**4**), and α2-$(SS)Cu_2Br_4$ (**5**) are polymers; **3** and **5** are one-dimensional and **4** has a corrugated 2D network. All the compounds contain corner-shared tetrahedra with Cu–Br–Cu connections, and in some cases, edge-shared with double bromine bridges. The copper coordination is tetrahedral, either $CuBr_4$ or $CuBr_3S$, except in one case, in which trigonal geometry was encountered. Compounds **1**, **2**, and **4**, which are synthesized at 50 °C, display Cu–S bonds with the cystamine through either one or both sulfur atoms. On the other hand, **3** and **5**, which are synthesized at 80 °C, do not have any. There is a high tendency to form hydrogen bonds between the polar ammonium heads of the cystamine with the bromine atoms. The range of phases experienced in this system is related to the bifunctional nature of cystamine, which is characterized by its primary ammonium ends and its disulfide bridge, and to the subtle competition between Br^- and S–S ligands towards the Cu^I ions, which appears to be controllable by temperature. The presence of both chiral M- and P-helicoidal conformers of cystamine in **1**–**5** results in racemic compounds adopting centrosymmetric structures for **1**, **3**, **4**, and **5** but **2** adopts a noncentrosymmetric structure ($P2_12_12_1$) resulting from the coordination of copper ions to one conformer; the other conformer is noncoordinated and acts as the counterion.

Introduction

One area of continuous activity in the chemistry and physics of materials deals with hybrid organic–inorganic systems as a result of the potential combination of properties of the two moieties within one compound that can be used as sensors. As such, the family of halogenometalates is of high interest. For instance, solution processing of such hybrids by using room-temperature techniques has been demonstrated.[1] Whereas molecules are also mainly responsible for nonlinear optical properties of some iodometalate salts,[2] the physical properties of these hybrid materials such as their semiconducting,[3] magnetic[4] or luminescence[5] properties usually arise from the inorganic part. Recently, we focused our attention on the synthesis of the halogenometalate of Bi^{III} and Pb^{II} hybrid materials containing the diprotonated cystamine molecule $[H_3N(CH_2)_2S–S(CH_2)_2NH_3]^{2+}$, denoted by SS. This molecular entity displays interesting features. First, the primary ammonium functionalities of this nonbulky cation are in favor of the formation of extended 1D or 2D inorganic networks in their corresponding salts. Secondly, in contrast to simple diammonium cations such as alkyldiammonium, the disulfide bridge can be involved in intermolecular interactions leading to unusual structures.[5a,6] Organic disulfide is also a moderate donor towards soft-metal ions, especially in the case of polyfunctional disulfide ligands that are well known to form complexes in biological systems or in synthetic model compounds.[7] Finally, cystamine molecules or derivatives, as known for disulfides RSSR′, show skewed structures in their crystalline states and both enantiomeric conformers exist; the dihedral angle formed by the intersection of the two planes defined by CSS and SSC′, respectively, are approximately 90°, which leads to chiral P- and M-helical forms.[8] In the case of spontaneous resolution (mixture of crystals of the two pure enantiomers), these conformationally chiral molecules can crystallize in enantiomorphous systems, which leads to nonlinear optical properties, as found for $(H_3O)(SS)PbI_5$.[5a]

The broad area of organic/inorganic cuprous halide salts continues to be fascinating for solid-state materials, as well as for biological systems. It includes the CuXL family[4d,9] combining copper(I) halide with monodentate or bidentate N ligands that display photoluminescence properties.[4d] Regarding the field of purely cuprous halide salts, it provides a wide area for structural research as a result of the diverse coordination modes of the Cu^I ion, as well as the multiple bridging capabilities of the halide ions. Thus, the $Cu^I_xX_y^{n-}$

[a] Laboratoire de Chimie, Ingénierie Moléculaire et Matériaux d'Angers, UMR-CNRS 6200, Université d'Angers,
2 Bd Lavoisier, 49045 Angers, France
Fax: +33-2-41735405
E-mail: nicolas.mercier@univ-angers.fr
[b] Laboratoire de Chimie de Coordination Organique, UMR-CNRS 7140, Université Louis Pasteur,
4 rue Blaise Pascal, 67000 Strasbourg, France

Supporting information for this article is available on the WWW under http://www.eurjic.org or from the author.

anions may form discrete geometries of varying nuclearity or polymeric extended systems.[10] The anion mode of aggregation of Cu^{+} and X^{-} with a given cation is not easy to predict, as the aggregation forces may be under kinetic control. However, it is interesting to note that, to date, extended structures have been essentially one dimensional; only two examples of two-dimensional networks have been reported.[11] Several kinds of cations were used in this chemistry, notably those with or without hydrogen-bonding capabilities. Owing to the hydrogen bonding capabilities added to the disulfide–copper bonding capabilities of diprotonated cystamine molecules, new constraints are placed in the system and this can lead to unusual and interesting structures.

By using the disulfide-based ammonium cations $[NH_3(CH_2)_2SS(CH_2)_2NH_3]^{2+}$, we investigated the chemistry of copper(I) salts that were well known to be easily formed by autoreduction of copper(II) in alcohol solvents or in water at elevated temperatures.[11b,12] We report here on the preparation and the crystal structures of five copper(I) salts, $(SS)_2Cu_4Br_8$ (**1**), $(SS)_2Cu_2Br_6$ (**2**), α1-$(SS)Cu_2Br_4$ (**3**), $(SS)Cu_3Br_5$ (**4**), and α2-$(SS)Cu_2Br_4$ (**5**). We will show that the disulfide parts of the cations are able to complex the copper(I) ions in **1**, **2**, **3**, and **4** to give either chiral molecular entities (**1**, **2**) or to participate in extended copper halide networks (1D in **3**, 2D in **4**). The formation of Cu–S bonds is not favored in reactions performed at elevated temperatures, as demonstrated by the structure of **5**, which is built up of $CuBr_2$ 1D chains.

Results and Discussion

Synthesis

Depending on the experimental conditions, five compounds containing diprotonated cystamine and bromocuprate(I) were prepared. Three of these compounds are polymorphs (**1**, **3**, and **5**) with the formula $(SS)Cu_2Br_4$ [note that **1** is written as $(SS)_2Cu_4Br_8$ because of the presence of tetrameric molecular entities in the structure], whereas **2** and **4** can be conceptually obtained by removing/adding one CuBr from/to $(SS)Cu_2Br_4$ for **2**/**4**, respectively. This wide variety of structures obtained with this multifunctional cation can be related to the known multiple bridging capabilities of the halide ions and especially to the competition between the Br and S–S ligands towards the soft metallic center (Cu^{I}). Thus, strong Cu–S bonds ($d \approx 3.30$ Å) are present in three of the five structures, which leads to copper(I) molecular complexes in the structure of **1** and **2** or to an extended 2D network as in **4**. In contrast, the structures of **3** and **5**, which were synthesized at elevated temperatures, display either no Cu–S bond in **5** or a weaker Cu–S bond ($d \approx 3.60$ Å) in **3**; the existence of this bond is additionally related to the occupation rate of 0.33 of the copper ions disordered over two positions. It must be noted that copper halide complexes based on simple disulfide ligands such as diethyl disulfide are quite scarce[13] relative to those based on polyfunctional disulfide multidentate ligands.[7] The formation of Cu–S(cystamine) bonds in **1**–**4** may be explained by the additional effect of the ammonium moiety of the cystamine cation, which interacts with the bromine atom through electrostatic forces and hydrogen bonding.

Structure of 1

The crystal structure of **1** is built from molecular tetrameric entities of $[(SS)_2Cu_4Br_8]$ (Figure 1) consisting of two dimeric halves fused together by two edge-sharing tetrahedra. A very interesting feature of this tetramer is that six of the eight bromine atoms are on one side and cystamine is on the opposite side; thus, the tetramer is expected to have a high dipole moment. More important is that the cystamine moieties are of the same helicoidal conformation, which means that each tetramer can be considered as a chiral entity (Figure 1b). The tetramer can also be described as two disulfide bridged (μ-bromo)dicopper(I) complexes connected through two bromine atoms. The disulfide bridged (μ-bromo)dicopper(I) complex, which can be reduced to the [–S–S–Cu–Br–Cu–] cycle, (Figure 1b) is quite rare. It was described recently as the result of the conversion of a bis(μ-thiolato)dicopper(II) complex mediated by halide ions.[7b] In **1**, every copper is tetrahedrally coordinated by one S atom [$d_{(Cu–S)}$ = 2.318(1) Å (Cu1) or 2.390(1) Å (Cu2)] and three Br atoms (Table 1). The Cu1 and Cu2 copper atoms bridged by disulfide are separated by 3.416(3) Å, whereas

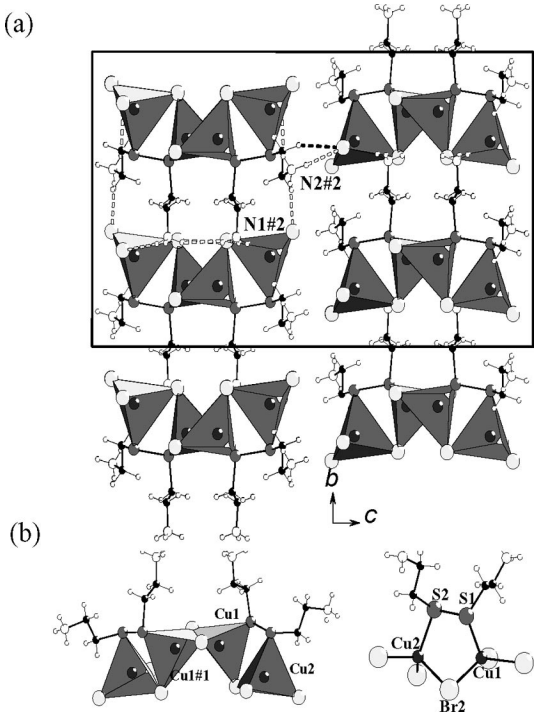

Figure 1. Structure of **1**: (a) general view along the *a* axis and hydrogen bonds involving one selected molecular entity [(N)H···Br and (C)H···Br in white dotted lines and black dotted lines respectively]; (b) molecular entity (left) and part of it showing the–S–S–Cu–Br–Cu–cycle (right), d[Cu(1)–Cu(1)#1] = 2.7213(14) Å (#1: $-x + 2$, y, $-z + 1/2$; #2 $1.5 - x$, $0.5 + y$, $0.5 - z$).

the distance between adjacent symmetry-related Cu1 atoms bridged by two bromide atoms is 2.721(1) Å. Such a short Cu···Cu contact is often observed in bromocuprate(I) salts.[10b] The existence of these polar units, and thus strong dipole–dipole interactions, and strong hydrogen bonding result in the stacking along the *b* direction of the tetramers in a head-to-tail arrangement. Thus, acentric sheets parallel to the *ab* plane can be defined. The hydrogen bonds involving the four ammonium parts of a selected molecular entity are drawn in Figure 1a. Of the 12 (N)H···Br contacts, 10 of them are in the range 2.44–2.71 Å and occur between entities along the *b* direction. Several hydrogen bonds are counted between molecules of neighboring sheets, especially an unusual (C)H···Br contact of 2.83 Å (Figure 1a). Finally, **1** crystallizes in the centric *C*2/*c* space group, and neighboring sheets are related by the *c* glide plane. We can wonder if these molecular entities exist in solution, or if they are formed during the crystallization process. Nevertheless, we note that rapid evaporation of the solution leads to **1**, which can be considered as kinetically controlled, whereas slow evaporation of the solution mainly leads to thermodynamically stable **4**.

Table 1. Selected bond distances and angles for **1**.

Atoms	Distance [Å]	Atoms	Angle [°]
Br(1)–Cu(1)	2.4363(9)	S(2)–S(1)–Cu(1)	101.88(7)
Br(2)–Cu(1)	2.4816(9)	S(1)–S(2)–Cu(2)	100.99(7)
Cu(1)–S(1)	2.3177(14)	Cu(1)–Br(2)–Cu(2)	84.52(3)
Cu(1)–Br(1)#1	2.5122(9)	S(1)–Cu(1)–Br(2)	95.97(4)
Br(3)–Cu(2)	2.4199(9)	S(2)–Cu(2)–Br(2)	106.89(4)
Br(2)–Cu(2)	2.5963(9)		

Structure of 2

The crystal structure of **2** is built from anionic dimers, $[(SS)Cu_2Br_6]^{2-}$, and noncoordinated diprotonated cystamine (Figure 2). The asymmetric dicopper(I) entities are formed by two kinds of tetrahedra, $CuBr_4$ and $CuBr_3S$, which are bridged by one bromine atom (Figure 2b). The bond distances are given in Table 2. As the result of the enantiomorphic $P2_12_12_1$ space group, all coordinated disulfide molecules on one hand, and all noncoordinated disulfide molecules on the other hand, have the same helicoidal conformation. Noteworthy is that both kinds of disulfide molecules display both helicoidal forms. To the best of our knowledge, compounds having two enantiomers of equal quantities crystallizing in a noncentrosymmetric space group are very scarce. The present case is helped by the fact that one enantiomer is coordinated and the other is noncoordinated, which serves to counterbalance the charges. Second-order nonlinear optical (NLO) properties, which are only observable in noncentrosymmetric materials, are detectable on the white powder sample of **2**. The measurements of the effective second-order susceptibility tensor were evaluated by using the approximative Kurtz–Perry method.[14] The measured second harmonic generation (SHG) efficiency was compared to that of POM (3-methyl-4-nitropyridine-1-oxide), which was used as a reference material for the powders. The ratio of the harmonic and fundamental intensities gives the conversion efficiency of the sample, and it was calculated from the following equation $\chi^{<2>}_{sample}/\chi^{<2>}_{POM} = (I^{SH}_{sample}/I^{SH}_{POM})^{1/2}$. Compound **2** shows a weak second-order nonlinear susceptibility of 0.1 pm V^{-1}, which is about 1 and 10% of the efficiency of POM and quartz, respectively.

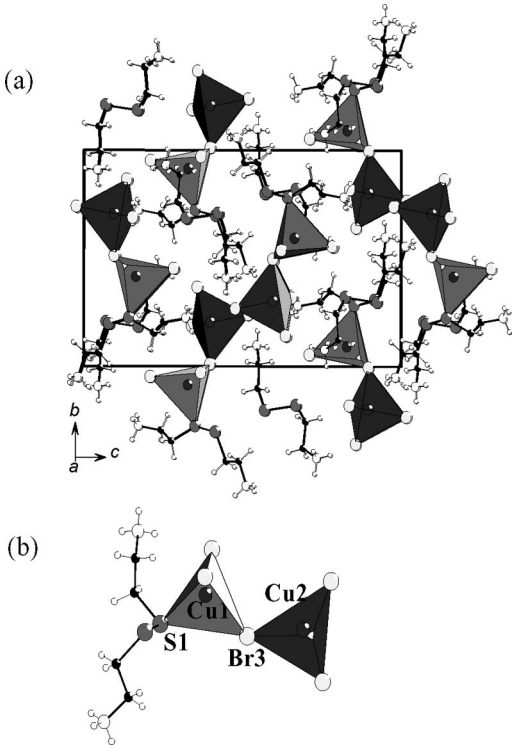

Figure 2. Structure of **2**: (a) general view along the *a* axis; (b) molecular entities of $[(SS)Cu_2Br_6]^{2-}$, $CuBr_4$, and $CuBr_3S$ drawn as dark-gray-colored and light-gray-colored tetrahedra, respectively.

Table 2. Selected bond distances [Å] for **2**.

Atoms	Distance [Å]	Atoms	Distance [Å]
Br(2)–Cu(1)	2.5002(10)	Br(4)–Cu(2)	2.4643(9)
Br(3)–Cu(1)	2.4890(9)	Br(5)–Cu(2)	2.4540(8)
Cu(1)–S(1)	2.3544(14)	Br(6)–Cu(2)	2.5000(10)
Cu(1)–Br(1)	2.4635(8)	Br(3)–Cu(2)	2.5264(9)

Structure of 3

The crystal structure of **3** is built from 1D inorganic chains running along the *c* axis and is separated by the cystamine cations (Figure 3). In the structure, Cu(1) is disordered over two positions (see Experimental Section), which implies two kinds of coordination for the copper ions: either a $CuBr_3S$ tetrahedral coordination (Cu1A, Figure 3a) or a nearly $CuBr_3$ triangular coordination (Cu1B, Fig-

ure 3b). The structure determination from data collected at room temperature leads to occupancy values of 0.33 and 0.67 for Cu1A and Cu1B, respectively, whereas the ratio becomes 0.50/0.50 at 150 K. When considering the Cu1B atom, the inorganic network is an unprecedented Cu_2Br_4 chain.[15] In the chain, consecutive pairs of copper (Cu2) edge-sharing tetrahedra are linked by two $Cu(1B)Br_3$ triangular entities (Figure 3b) through one terminal bromine atom of one dimer and a bridging bromine atom of another pair. Note that the Cu1B atom that is bonded to three nearby bromine atoms (average distance of 2.405 Å) also weakly interacts with another bromine atom at a distance of 3.007(7) Å (Table 3). A coordination of 3+1 appears to be more appropriate. The distances between copper centers are longer than 3.0 Å. Especially, the Cu1B···Cu2 distance of 3.015(5) cannot explain the preferential occupation of the Cu1A site by Cu1 atoms at low temperatures as a result of hypothetical Cu1B···Cu2 repulsion forces. Considering the Cu1A site, one can consider a tetrahedral coordination for Cu1A atoms with three bromine atoms (average distance of 2.478 Å, see Table 3) and one sulfur atom (d = 2.638 Å). The 1D inorganic network with the formulation of Cu_2Br_4S can be described as pairs of copper (Cu2) edge-sharing tetrahedra sharing Br corners with four neighboring $CuBr_3S$ tetrahedra (Figure 3a).

Table 3. Selected bond distances [Å] for **3**.

Atoms	Distance [Å]	Atoms	Distance [Å]
Br(2)–Cu(1A)	2.578(4)	Br(2)–Cu(1B)	2.480(2)
Br(1)–Cu(1A)	2.360(4)	Br(1)–Cu(1B)	2.400(3)
Cu(1A)–Br(3)#3[a]	2.498(5)	Cu(1B)–Br(3)#3	2.334(3)
S(1)–Cu(1A)	2.638(7)		
Cu(2)–Br(4)	2.3893(15)	Br(3)–Cu(2)	2.4003(16)
Cu(2)–Br(2)#1	2.5357(16)	Br(2)–Cu(2)	2.6160(17)

[a] #1 $-x + 1, -y + 1, -z + 1$; #2 $x, y, z - 1$; #3 $x, y, z + 1$.

Structure of 4

The crystal structure of **4** is built from a two-dimensional inorganic lattice (Figure 4). The asymmetry unit consists of one independent cystamine units, three copper ions, and

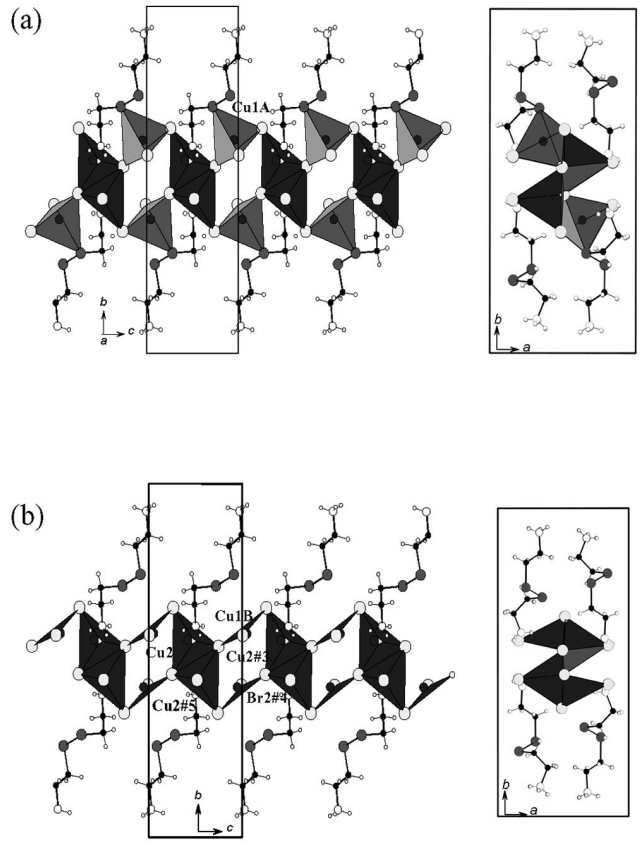

Figure 3. Part of the structure of **3**, which shows the 1D inorganic network along the *a* (left) and *c* (right) directions in the case of (a) [Cu*1a*Br_3S] tetrahedral coordination of Cu*1a* (33% occupation rate, light-gray-colored tetrahedra); (b) [Cu*1b*Br_3] triangular coordination of Cu*1b* (67% occupation rate); d[Cu(1B)–Cu(2)#3] = 3.015(5) Å, d[Cu(1B)–Br2#4] = 3.007(7) Å, d[Cu(2)–Cu(2)#5] = 3.517(7) Å (#3 $x, y, z + 1$; #4 $1 - x, 1 - y, 2 - z$; #5 $1 - x, 1 - y, 1 - z$).

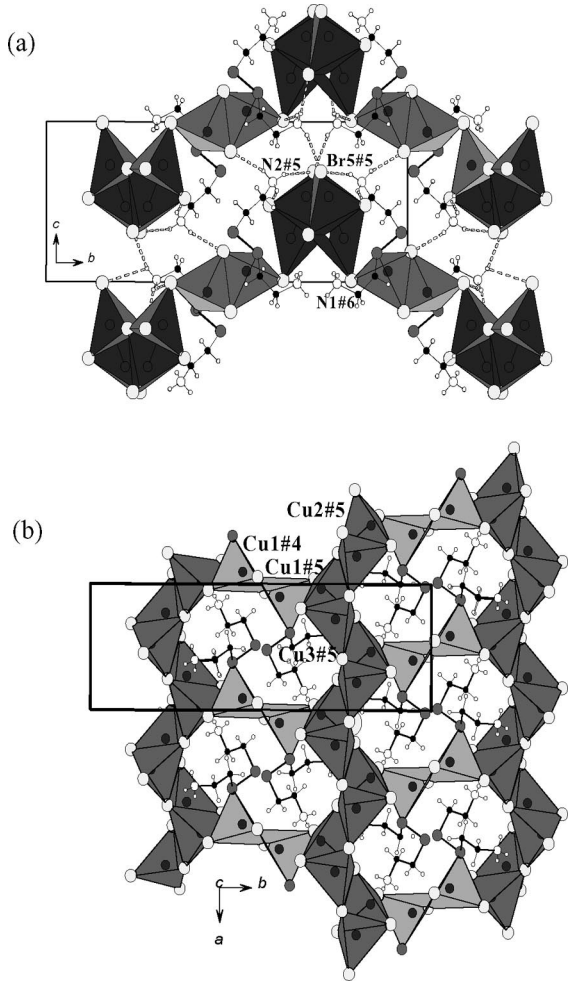

Figure 4. The layered structure of **4**: (a) general view along the *a* axis showing the interlayer hydrogen bonding; (b) part of the structure showing the open two-dimensional network; d[Cu(1)#4–Cu(1)#5] = 2.9822(18) Å, d[Cu(3)#5–Cu(2)#5] = 2.7740(15) Å, (#4 $0.5 - x, 0.5 + y, -z$; #5 $x - 0.5, 0.5 - y, z$, #6 $x, 1 + y, z$); $CuBr_4$ and $CuBr_3S$ drawn as dark-gray-colored and light-grey-colored tetrahedra, respectively.

five bromine atoms. Cu2 and Cu3 are tetrahedrally coordinated by four bromine atoms (bond distances in Table 4, dark-gray-colored polyhedra in Figure 4). They build chains along the *a* axis that can be defined as pairs of copper edge-sharing tetrahedra bridged together by two corners. The coordination of Cu1 is also tetrahedral: one sulfur atom of the disulfide is linked with a distance of 2.278(1) Å and the average Cu–Br bond length is 2.488 Å (Table 4, light-gray-colored polyhedra in Figure 4). The chains of $CuBr_4$ tetrahedra running along the *a* direction and the pairs of edge-sharing $CuBr_3S$ tetrahedra are linked together and in so doing define the unprecedented Cu_3Br_5S open two-dimensional framework (Figure 4b). Ten bridged $CuBr_4$ or $CuBr_3S$ tetrahedra define windows that accommodate the cystamine molecules. More precisely, the molecules lie down inside the windows, and each of their ammonium parts are located at each side of the inorganic sheet in the interlayer space. The hydrogen bonds are drawn in Figure 4a for (N)H···Br distances inferior to 2.95 Å. Each–$N(1)H_3$ or –$N(2)H_3$ ammonium part of the cystamine cations belonging to a given sheet interacts with two bromine atoms of this sheet and with another of the neighboring sheet. We can also note that the terminal Br5 bromine atoms are stabilized by a set of hydrogen bonds given by both –$N(1)H_3$ or –$N(2)H_3$ parts.

Table 4. Selected bond distances [Å] for **4**.

Atoms	Distance [Å]	Atoms	Distance [Å]
Br(1)–Cu(1)	2.4137(11)	Br(3)–Cu(2)	2.3908(13)
Br(2)–Cu(1)	2.5574(11)	Br(4)–Cu(2)	2.7940(14)
Cu(1)–S(1)	2.2777(17)	Br(2)–Cu(2)	2.4002(13)
Cu(1)–Br(1)#1[a]	2.4943(12)	Br(4)–Cu(2)#2	2.5297(12)
Br(3)–Cu(3)	2.4263(11)	Br(5)–Cu(3)	2.5483(12)
Br(4)–Cu(3)	2.5195(12)	Cu(3)–Br(5)#2	2.4846(11)

[a] #1 $-x + 1, -y, -z$; #2 $x + 1/2, -y - 1/2, z$; #3 $x - 1/2, -y - 1/2, z$.

Structure of 5

The crystal structure of **5** consists of noncoordinated cystamine molecules and $CuBr_2$ chains that form an elegant tetragonal arrangement (Figure 5). The $CuBr_2$ chains are built from edge-shared tetrahedra. This kind of chain is not unique, as other bromocuprate salts containing such a chain have already been reported.[15] Moreover, we can notice that this kind of polymeric anion is inclined to give tetragonal symmetry as observed for **5**, which crystallizes in the $I4_1/a$ space group.[15b–15d] In **5**, consecutive molecules along the *c* axis are approximately perpendicular to each other as underlined by the relative positions of their disulfide bridge (Figure 5). Finally, the structure may be regarded as if the cystamine molecules define a square porous-like organic network that is filled with $CuBr_2$ chains. The range of Cu–Br bond lengths is 2.475(1)–2.541(1) Å in the $CuBr_4$ tetrahedra (Table 5), whereas a distance of 2.801(1) Å is observed between neighboring copper ions. This is due to hydrogen bonding between the ammonium parts of cystamine and the bromine atoms and to consecutive tetrahedra that are tilted in such a way that the Cu–Cu–Cu angles are 161.0(1)°; thus gives rise to the distorted chains.

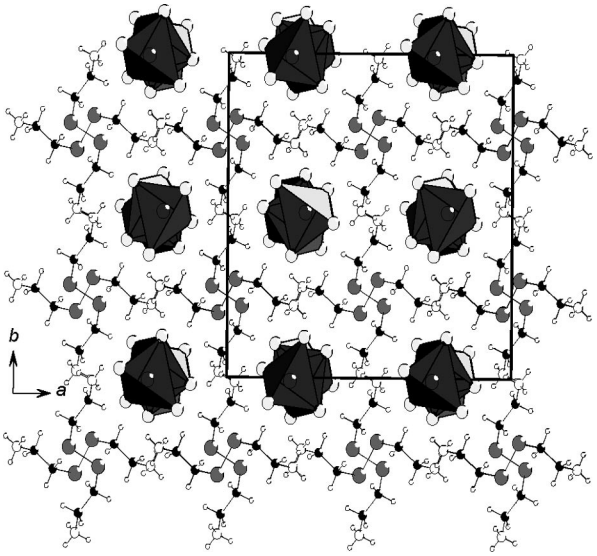

Figure 5. General view along the *c* axis of the structure of **5**; disorder on molecules not shown.

Table 5. Selected bond distances for **5**.

Atoms	Distance [Å]	Atoms	Distance [Å]
Cu–Br(1)	2.5135(10)	Cu–Br(2)	2.4753(10)
Cu–Br(1)#2[a]	2.5409(10)	Cu–Br(2)#1	2.5233(10)

[a] #1 $y - 1/4, -x + 7/4, z - 1/4$; #2 $-y + 7/4, x + 1/4, z + 1/4$.

Conclusions

We have established the use of the drug cystamine as a ligand for Cu^I and as a counterion within the same structure. The variety of structural phases obtained in this system relates to the competition between the Br and S atom for coordination with the Cu^I centers. Furthermore, one of these structural phases containing both enantiomers serendipitously crystallizes in a noncentrosymmetric space group. This fortuitous accident is due to the different crystallographic sites occupied by the pair of enantiomers. Further work in this area includes the use of other metal cations or the combination of Cu^I with other metal cations (as transition metal) to potentially add new properties (magnetism in the case of transition-metal cations) to the compounds so that they may be used as multifunctional materials.

Experimental Section

Chemicals: All starting compounds were obtained from commercial sources and used without purification.

(SS)$Cu^{II}Br_4$: Compounds **2**, **4**, and **5** were prepared from (SS)-$Cu^{II}Br_4$, and **3** from $CuBr_2$, by reduction with methanol by using different thermal techniques and procedures. (SS)$Cu^{II}Br_4$ was prepared by a solvothermal method by using a Teflon-lined PARR autoclave (internal volume: 25 mL). Hydrobromic acid (48%, 5 mL, *Fw* = 80.92, *d* = 1.49) was added to equimolar quantities of $Cu^{II}Br_2$ (134.02 mg, *Fw* = 223.36) and H_2N–CH_2–CH_2–S–S–CH_2–CH_2–NH_2·2HCl (97%, 135.12 mg, *Fw* = 225.2). After the heating–cooling steps (2 h from room temperature to 85 °C, 4 h at 85 °C, then 15 h from 85 °C to room temperature), very thin dark-purple plate crystals of (SS)$Cu^{II}Br_4$ were collected by filtration, washed with cold ethyl acetate, and kept at 40 °C to prevent moisture from being introduced. $C_4H_{14}Br_4CuN_2S_2$ (**1**) (537.45): calcd. C 8.94, Br 59.47, Cu 11.82, N 5.21, S 11.93; found C 9.21, Br 57.81, Cu 11.72, N 5.18, S 11.71 (Cl < 0.1).

(SS)$_2Cu_2Br_6$ (2): (SS)$Cu^{II}Br_4$ (150–160 mg) was dissolved in methanol (~3 mL). Copper(I) ions were formed by autoreduction of copper(II) in methanol. The mixture was stirred and heated on a hot plate at reflux for 2–3 min and then filtered, and the resulting dark-green solution was allowed to slowly evaporate in air for 1–2 d. Colorless crystals of **2** were collected by filtration and washed with cold ethyl acetate.

(SS)Cu_3Br_5 (4): A solution prepared according to the procedure for the synthesis of **2** was placed in a Teflon-lined PARR autoclave and heated in an oven at 50 °C for 12 h. The vessel was then cooled down rapidly. The resulting solution was filtered and colorless crystals of **4** were obtained and washed with cold ethyl acetate.

α2-(SS)Cu_2Br_4 (5): A solution prepared according to the procedure for the synthesis of **2** was placed in a Teflon-lined PARR autoclave and heated in an oven at 80 °C for 12 h and then was cooled down rapidly. After filtration, big colorless crystals of **5** as the main phase, and a small amount of crystals of **3** were obtained and washed with cold ethyl acetate. Crystals of **5** were selected by hand under a binocular microscope.

(SS)$_2Cu_4Br_8$ (1): Compound **1** was prepared by slow evaporation of an aqueous solution of $Cu^{II}Br_2$ (2 g, *Fw* = 223.36), H_2N–CH_2–CH_2–S–S–CH_2–CH_2–NH_2·2HCl (97%, 3 g, *Fw* = 225.2), and HBr (48%, 1.266 mL, *Fw* = 80.92, *d* = 1.49). The copper bromide was dissolved in distilled water (5 mL) and hydrobromic acid (1.266 mL). The cystamine salt was dissolved in distilled water (5 mL) and then added to the previous solution. The resulting mixture was stirred and heated to 50 °C for 1 h before it was rapidly filtered. The mixture was then cooled to room temperature. Colorless-to-pale yellow diamond-like crystals of **1** as the main phase and a small amount of crystals of **4** were obtained within 2–3 h. The crystals were collected by filtration and finally washed with cold ethyl acetate. Crystals of **1** were selected by hand under a binocular microscope.

α1-(SS)Cu_2Br_4 (3): Compound **3** was prepared under solvothermal conditions in a Teflon-lined PARR autoclave. Methanol (4 mL) and HBr (48%, 3.4 mL, 30 mmol, *Fw* = 80.92, *d* = 1.49) were added to $Cu^{II}Br_2$ (134.02 mg, *Fw* = 223.36) and H_2N–CH_2–CH_2–S–S–CH_2–CH_2–NH_2·2HCl (97%, 202.68 mg, *Fw* = 225.2). The autoclave was heated in a programmed oven with the following parameters: 2 h from room temperature to 85 °C, 2 h at 85 °C, then 12 h from 85 °C to room temperature. Colorless crystals of **3** were collected by filtration and washed with cold ethyl acetate.

The use of $Cu^{I}Br$ and/or an excess amount of HBr as starting materials did not give new phases, and only phases of **3** and **4** were obtained.

Thermal Analyses: Thermogravimetric analysis measurements, which consist of a 10 °C min^{-1} ramp from 25 to 900 °C under a flowing nitrogen atmosphere, were carried out by using a TGA-2050 Instruments System. Differential scanning calorimetry (DSC) measurements were performed with a DSC-2010 TA Instruments system. TGA measurements show that the compounds decompose in two steps with a first weight loss at about 200 °C for all **1**–**5** and a second weight loss at higher temperatures. As known in such hybrids, the first step probably corresponds to the departure of organic molecules together with HBr, whereas the second step corresponds to the sublimation of the remaining CuBr. On DSC curves, endothermic peaks are observed in the range 150–200 °C corresponding to melting or melting/solid state decomposition, before decomposition near 200 °C.

X-ray Crystallography: Powder X-ray diffraction measurements were carried out with a D8 Bruker diffractometer by using Cu-$K_{\alpha 1,2}$ radiation and a linear Vantec super-speed detector. Powder X-ray patterns of the homogeneous samples of **1**–**5** showed that all reflections are indexed in the unit cells obtained from X-ray diffraction of the single-crystal studies (see Supporting Information). X-ray diffraction data of selected single crystals were collected with a Bruker–Nonius KAPPA-CCD diffractometer equipped with graphite-monochromated Mo-K_α radiation (λ = 0.71073 Å). A summary of crystallographic data and refinement results for compounds **1**–**5** are given in Table 6. The structures were solved and refined by using the SHELXL97 package. Heavy atoms (Cu, Br, S) were first located by using direct methods, and C and N atoms were then located from the analysis of the Fourier difference maps. A statistical disorder affects one copper ion in the structure of **3**. Two positions were defined, and the occupancy of each was first refined by using isotropic thermal parameters constrained to be equal. Finally, the refinement of occupancy of disordered atoms with aniso-

Table 6. Crystallographic data for (SS)$_2Cu_4Br_8$ (**1**), (SS)$_2Cu_2Br_6$ (**2**), α1-(SS)Cu_2Br_4 (**3**), (SS)Cu_3Br_5 (**4**), and α2-(SS)Cu_2Br_4 (**5**).

	1	**2**	**3**	**4**	**5**
Fw [g mol^{-1}]	1202.02	915.12	601.01	744.46	601.01
Space group	*C*2/*c*	$P2_12_12_1$	$P2_1$/a	$P2_1$/a	$I4_1$/a
a [Å]	7.7957(8)	10.2558(7)	10.0661(9)	7.8248(8)	16.562(1)
b [Å]	14.755(1)	12.1174(7)	22.008(3)	22.909(2)	16.562(1)
c [Å]	25.212(3)	20.264(2)	6.6746(6)	9.3890(9)	10.893(1)
β [°]	93.40(1)	90	96.91(1)	108.04(1)	90
V [Å^3]	2894.9(8)	2518.3(3)	1467.9(3)	1600.3(5)	2987.9(2)
Z	4	4	4	4	8
Observed refl. [$I > 2\sigma(I)$]	2641	3866	1655	2777	1295
Parameters	130	219	141	148	78
R_1 [$I > 2\sigma(I)$]	0.042	0.039	0.044	0.050	0.043
wR_2 (all data)	0.083	0.052	0.126	0.120	0.088

tropic thermal parameters leads to a 0.33/0.67 ratio (see main text). In the structure of **5**, a disorder affects the C–S–S–C parts of molecules. The S atom and the C atom bonded to S were disordered over two positions. First, the occupancy of each part (C1A–S1A and C1B–S1B) was refined with the isotropic thermal parameters of S1A and S1B, and C1A and C1B, constrained to be equal, leading to $\tau = 0.8$ for the C1A–S1A part. Finally, all C and S atoms were refined anisotropically, the occupancies of two disordered parts were fixed to 0.8 and 0.2, respectively. All hydrogen atoms were treated with a riding model in all five structures. Positions and anisotropic displacement parameters of the non-H atoms were refined by full-matrix least-squares routines against F^2. Absorption effects were corrected by using the Gauss method or the SADABS method. Selected bond distances and angles for **1**–**5** are provided in Tables 1–5. CCDC-668343, -668344, -668345, -668346, and -668347 contain the supplementary crystallographic data for this paper. These data can be obtained free of charge from The Cambridge Crystallographic Data Centre via www.ccdc.cam.ac.uk/data_request/cif.

Non-Linear Optical Properties: The optical SHG was performed on powders by using the Kurtz and Perry method. The fundamental excitation wavelength at 1064 nm was provided by a Q-switch Nd:YAG laser (Model Continuum Leopard D-10) at a pulse duration of 16 ps and an average density power of 0.2 mJ per pulse for the repetition frequency of 10 Hz. The power of the fundamental beam was varied with a half-wave plate and a Glan polarizer. The beam was focused on the sample by a convergent lens having a focal length of 250 mm. The sample was rotated by using a stepped motor monitored by a power station of acquisition with an angle resolution up to 0.04°. The SH signal was detected by a photomultiplier tube (Hamamatsu $R_1$828-01), then integrated by a boxcar integrator and processed by a computer. Crystals of $(SS)_2Cu_2Br_6$ (**2**) were crushed and sieved in order to assure a crystallite size in the range 125–250 μm and then placed between two microscope slides.

Supporting Information (see footnote on the first page of this article): Powder X-ray patterns for **1**–**5**, thermal analysis (TGA, DSC), and experimental setup of the SHG experiment.

Acknowledgments

We thank Jerôme Luc and Bouchta Sahraoui (POMA Laboratory, University of Angers) for NLO measurements. This work was supported by the CNRS (France).

[1] a) D. B. Mitzi, *Chem. Mater.* **2001**, *13*, 3283; b) D. B. Mitzi, *J. Mater. Chem.* **2004**, *14*, 2355; c) E. Cariati, R. Ugo, F. Cariati, D. Roberto, N. Masciocchi, S. Galli, A. Sironi, *Adv. Mater.* **2001**, *13*, 1665; d) S. Sourisseau, N. Louvain, W. Bi, N. Mercier, D. Rondeau, F. Boucher, J. Y. Buzare, C. Legein, *Chem. Mater.* **2007**, *19*, 600.

[2] a) N. Mercier, A. L. Barres, M. Giffard, I. Rau, F. Kajzar, B. Sahraoui, *Angew. Chem. Int. Ed.* **2006**, *45*, 2100; b) A. M. Guloy, Z. Tang, B. Mirana, V. I. Srdanov, *Adv. Mater.* **2001**, *13*, 833; c) E. Cariati, D. Roberto, R. Ugo, P. C. Ford, S. Galli, A. Sironi, *Inorg. Chem.* **2005**, *44*, 4077.

[3] a) D. B. Mitzi, K. Chondroudis, C. R. Kagan, *IBM. J. Res. & Dev.* **2001**, *45*, 29; b) C. R. Kagan, D. B. Mitzi, K. Chondroudis, *Science* **1999**, *286*, 945; c) Z. Xu, D. B. Mitzi, C. D. Dimitrakopoulos, K. R. Maxcy, *Inorg. Chem.* **2003**, *42*, 2031; d) D. B. Mitzi, C. D. Dimitrakopoulos, L. L. Kosbar, *Chem. Mater.* **2001**, *13*, 3728; e) D. B. Mitzi, C. D. Dimitrakopoulos, J. Rosner, D. R. Meideros, Z. Xu, C. Noyan, *Adv. Mater.* **2002**, *14*, 1772.

[4] a) L. J. de Jongh, A. R. Miedema, *Adv. Phys.* **1974**, *23*, 1; b) R. Willet, H. Place, M. Middleton, *J. Am. Chem. Soc.* **1988**, *110*, 8639; c) G. S. Long, M. Wei, R. D. Willet, *Inorg. Chem.* **1997**, *36*, 3102; d) C. Bellito, P. Day, *J. Mater. Chem.* **1992**, *2*, 265.

[5] a) X. Hong, T. Ishihara, A. V. Nurmikko, *Phys. Rev. B* **1992**, *45*, 6961; b) T. Ishihara, *J. Luminescence* **1994**, *60–61*, 269; c) M. Era, S. Morimoto, T. Tsutsui, A. Saito, *Appl. Phys. Lett.* **1994**, *65*, 676; d) P. C. Ford, E. Cariati, J. Bourassa, *Chem. Rev.* **1999**, *99*, 3625.

[6] a) N. Louvain, W. Bi, N. Mercier, J. Y. Buzaré, C. Legein, G. Corbel, *Dalton Trans.* **2007**, 965; b) W. Bi, N. Louvain, N. Mercier, J. Luc, B. Sahraoui, *CrystEngComm* **2007**, *9*, 298.

[7] a) T. Osako, Y. Ueno, Y. Tachi, S. Itoh, *Inorg. Chem.* **2003**, *42*, 8087; b) Y. Ueno, Y. Tachi, S. Itoh, *J. Am. Chem. Soc.* **2002**, *124*, 12428; c) S. Itoh, M. Nagagawa, S. Fukuzumi, *J. Am. Chem. Soc.* **2001**, *123*, 4087; d) L. G. Warner, T. Ottersen, K. Seff, *Inorg. Chem.* **1974**, *13*, 2819; e) T. Ottersen, L. G. Warner, K. Seff, *Inorg. Chem.* **1974**, *13*, 1904.

[8] a) R. Steudel, *Angew. Chem. Int. Ed. Engl.* **1975**, *14*, 655; b) J. Webb, R. W. Stickland, F. S. Richardson, *J. Am. Chem. Soc.* **1973**, *95*, 4775; c) G. Gottarelli, B. Samori in *The Chemistry of Ethers, Crown Ethers, Hydroxyl Groups and their Sulphur Analogues* (Ed.: A. Patai), Wiley, New York, **1980**, p. 279; d) R. Steudel, Y. Drizdova, K. Miaskiewick, R. H. Hertwig, W. Koch, *J. Am. Chem. Soc.* **1997**, *119*, 1990.

[9] a) P. M. Graham, R. D. Pike, *Inorg. Chem.* **2000**, *39*, 5121; b) F. Thebault, S. A. Barnett, A. J. Blake, C. Wilson, N. R. Champness, M. Schröder, *Inorg. Chem.* **2006**, *45*, 6179; c) L. R. Hanton, R. M. Hellyer, M. D. Spicer, *Inorg. Chim. Acta* **2006**, *359*, 3659.

[10] a) From the CCDC, about twelve types of discrete entities ranging from mononuclear CuX_3 (X = Br, I, Cl) to polynuclear (e.g., Cu_8Br_{15} or $Cu_{10}I_{15}$), about ten types of one-dimensional polymeric networks, and a couple of two-dimensional networks were reported, see also: b) Bonding in halocuprates: L. Subramanian, R. Hoffmann, *Inorg. Chem.* **1992**, *31*, 1021.

[11] a) H. Place, B. Scott, G. S. Long, R. D. Willet, *Inorg. Chim. Acta* **1998**, *279*, 1; b) R. D. Willet, *Inorg. Chem.* **2001**, *40*, 966.

[12] R. D. Willet, B. Twamley, *Inorg. Chem.* **2004**, *43*, 954.

[13] a) P. M. Boorman, K. A. Kerr, R. A. Kydd, K. J. Moynihan, K. A. Valentine, *J. Chem. Soc., Dalton Trans.* **1982**, 1401; b) S. Le Moustarder, N. Mercier, P. Hudhomme, N. Gallego-Planas, A. Gorgues, A. Riou, *Synt. Met.* **2002**, *130*, 129.

[14] a) S. K. Kurtz, T. T. Perry, *J. Appl. Phys.* **1968**, *39*, 3798; b) K. Sankaranarayanan, P. Ramasamy, *Cryst. Res. Technol.* **2006**, *41*, 225.

[15] The $CuBr_2$ chains that were described consist of edge-shared tetrahedra: a) R. Fletcher, J. J. Hansen, J. Livermore, R. D. Willet, *Inorg. Chem.* **1983**, *22*, 330; b) B. Scott, R. Willet, L. Porter, J. Williams, *Inorg. Chem.* **1992**, *31*, 2483; c) J. Sertuka, A. Luque, F. Loret, P. Roman, *Polyhedron* **1999**, *17*, 3875; d) T. Matsumoto, Y. Kamada, T. Sugimoto, T. Tada, H. Nakazumi, T. Kawakami, K. Yamaguchi, *Synth. Met.* **2003**, *135*, 575.

Received: November 21, 2007
Published Online: February 19, 2008

